



# Hydrogen-bonded macrocycle-mediated dimerization for orthogonal supramolecular polymerization

Wentao Yu, Zhiyao Yang, Chengkan Yu, Xiaowei Li\* and Lihua Yuan\*

## Full Research Paper

Open Access

Address:  
College of Chemistry, Sichuan University, Chengdu 610064, China

Email:  
Xiaowei Li\* - lixw@scu.edu.cn; Lihua Yuan\* - lhyuan@scu.edu.cn

\* Corresponding author

Keywords:  
hydrogen-bonded macrocycle; orthogonal self-assembly;  
shape-persistent; supramolecular polymer

*Beilstein J. Org. Chem.* **2025**, *21*, 179–188.  
<https://doi.org/10.3762/bjoc.21.10>

Received: 19 October 2024  
Accepted: 09 January 2025  
Published: 17 January 2025

This article is part of the thematic issue "Emerging directions in supramolecular chemistry".

Guest Editors: J. W. Meisel and A. H. Flood



© 2025 Yu et al.; licensee Beilstein-Institut.  
License and terms: see end of document.

## Abstract

Orthogonal self-assembly represents a useful methodology to construct supramolecular polymers with AA- and AB-type monomers, as commonly used for covalently linked polymers. So far, the design of such monomers has relied heavily on three-dimensional macrocycles, and the use of two-dimensional shape-persistent macrocycles for this purpose remains rather rare. Here, we demonstrate a dimerization motif based on a hydrogen-bonded macrocycle that can be effectively applied to form orthogonal supramolecular polymers. The macrocycle-mediated connectivity was confirmed by single-crystal X-ray diffraction, which revealed a unique 2:2 binding motif between host and guest, bridged by two cationic pyridinium end groups through  $\pi$ -stacking interactions and other cooperative intermolecular forces. Zinc ion-induced coordination with the macrocycle and a terpyridinium derivative enabled orthogonal polymerization, as revealed by  $^1\text{H}$  NMR, DLS, and TEM techniques. In addition, viscosity measurements showed a transition from oligomers to polymers at the critical polymerization concentration of 17  $\mu\text{M}$ . These polymers were highly concentration-dependent. Establishing this new dimerization motif with shape-persistent H-bonded macrocycles widens the scope of noncovalent building blocks for supramolecular polymers and augurs well for the future development of functional materials.

## Introduction

Host–guest interactions, particularly those involving macrocycles as hosts [1], have found a myriad of applications in supramolecular chemistry [2–4] owing to their ability to create noncovalent, dynamic, yet in some cases strong forces between molecules. Adding an additional element of interactions to supramolecular systems endows them with a feature of “orthogonal self-assembly”, a process in which molecular species are

assembled into aggregates by two or more types of noncovalent interactions that work independently from each other [5–8]. Generating such motifs with orthogonal propensity is appealing not only for the construction of supramolecular polymers with the ability to modulate their structure and properties in multiple ways through adjustment of noncovalent bonding interactions. It also confers on supramolecular assemblies with higher com-

plexity and multilevel ordering [9–11], leading to a vast number of applications, for example, for use in detection and separation [12], sensing [13], photocatalysis [14], release [15], and as thermochromic and photoluminescent materials [16]. In this regard, macrocycles emerged a decade ago as a “sticking” end for homo- and heterodifunctional monomers, enabling supramolecular polymerization [17]. So far, macrocycles that are applied to orthogonal self-assembly have been limited to three-dimensional rings, such as cucurbituril [18], cyclodextrin [19], and calix[4]pyrrole [20], as well as flexible crown ethers [10,21]. Few two-dimensional (2D) shape-persistent macrocyclic compounds are used for this purpose. One difficulty in realizing 2D macrocycle-based orthogonal assembly is that the construction motif must be capable of dimerization by binding to a macrocycle in a 2:2 stoichiometry [22,23]. Such binding motifs are intriguing for macrocycle-mediated supramolecular dimerization since they may enable multiple modes of noncovalent connectivity through combination with other noninterfering interactions (e.g., metal coordination interactions and hydrogen bonding), providing access to various multiresponsive orthogonal self-assemblies or smart supramolecular polymers [24,25]. For example, the discovery of cucurbit[8]uril complexation in a 1:2 and 2:2 host–guest stoichiometry leads to a wide spectrum of applications, which includes catalysis [26], gelation [27], sensing [28], color tuning, etc. [29]. However, only several kinds of macrocycles are capable of supramolecular dimerization through host–guest interactions [30].

Shape-persistent macrocycles have captured the interest of chemists for decades [31,32]. This is not only due to their rich host–guest chemistry but also due to  $\pi$ -surface-enabled self-assembly that enables the creation of various supramolecular structures, such as discotic liquid crystals [33], nanodimers [34], and organic frameworks [35]. Among them, shape-persistent hydrogen-bonded aromatic amide macrocycles [36–42], a class of cyclic compounds comprising a number of aromatic residues with consecutive intramolecular hydrogen bonds and amide linkages, stand out as versatile host molecules as their cavity size, peripheral side chains, and recognition sites are tunable to suit desired functions. These macrocycles have found widespread applications owing to their unique host–guest behaviors in the fields of recognition [43], ion channels [44], catalysis [45], rotaxanes [46], as well as molecular machines [47]. We envisioned that the use of a H-bonded aromatic amide macrocycle with six aromatic residues (hereafter called cyclo[6]aramide for brevity, Scheme 1a) could mediate dimerization as a host. That is because such a 2D macrocycle has six carbonyl oxygen atoms pointing inwards as binding sites, demonstrating excellent affinity for cationic organic guests, including pyridinium and its derivatives [40]. More importantly, it favors intermolecular  $\pi$ -stacking interactions with aromatic

guests [48]. Herein, we report on a novel supramolecular dimerization motif in 2:2 stoichiometry using H-bonded aramide macrocycles for constructing orthogonal supramolecular polymers (Scheme 1).

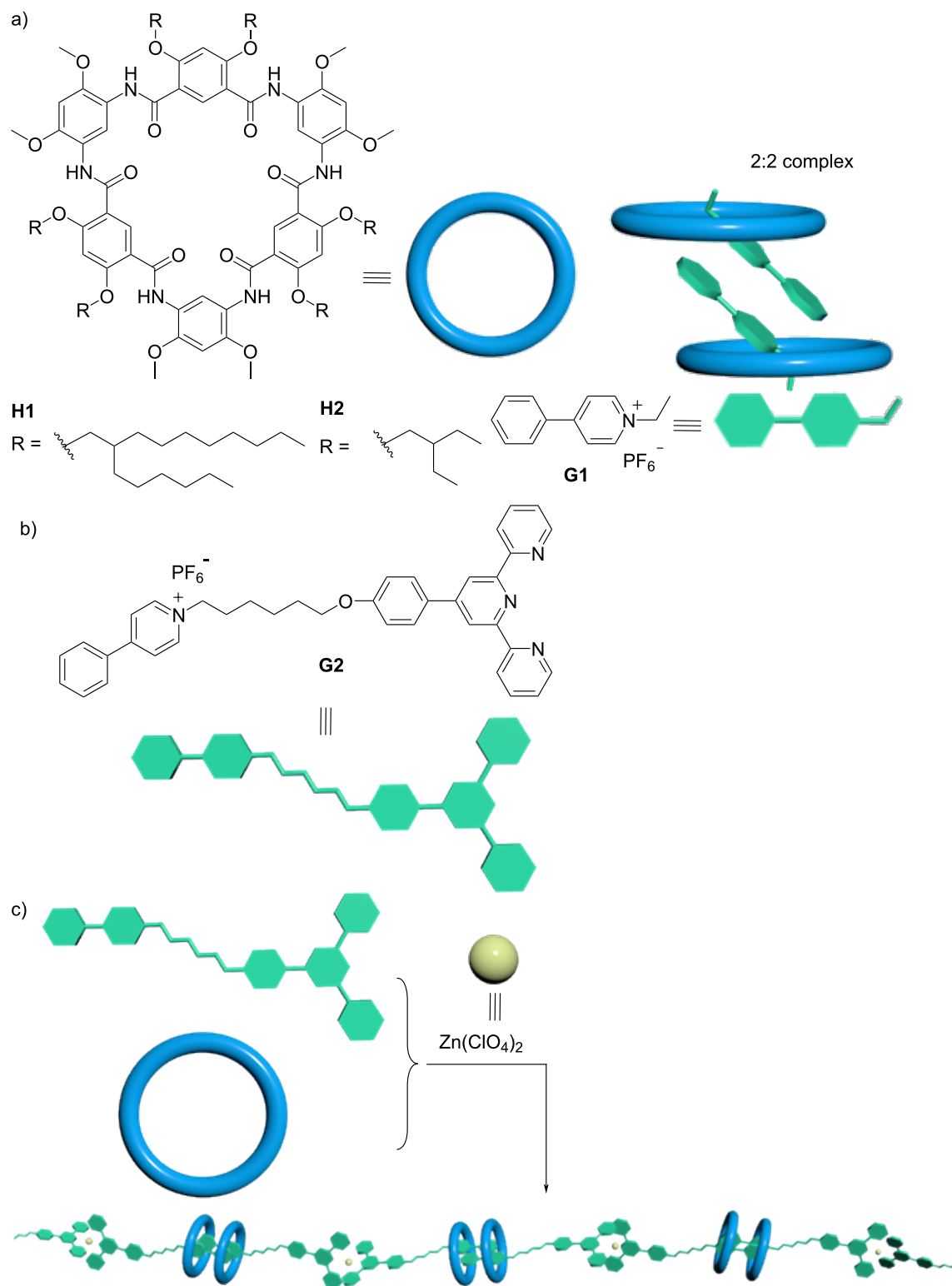
The terpyridyl group and the pyridinium cation in the AB-type monomer **G2** each function as a “sticker” to enable supramolecular polymerization in the presence of the macrocyclic component and zinc ions. The driving force for the recognition involves multiple cooperative interactions, particularly  $\pi$ -stacking interactions between the aromatic rings in a parallel fashion from both host and guest, which is demonstrated by the crystal structure of the key element of the recognition motif.

## Results and Discussion

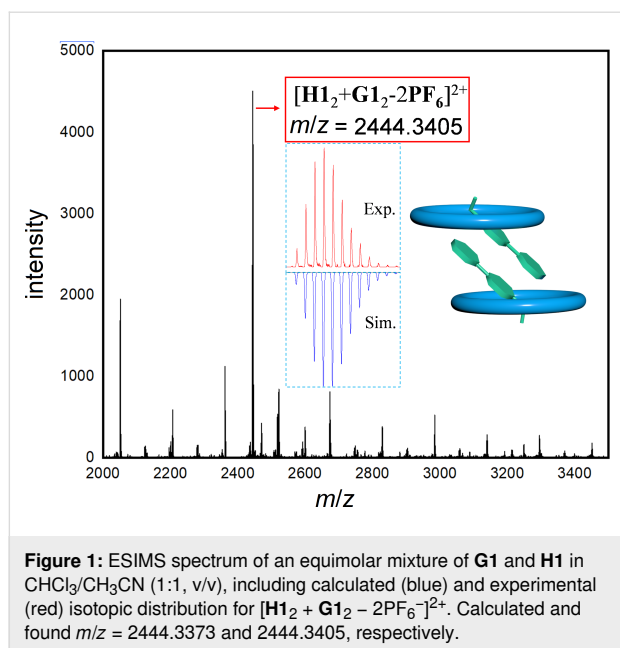
### Backdrop for design considerations

Our interest in macrocycle-mediated supramolecular dimerization was triggered by observations in mass spectrometry experiments when exploring host–guest interactions. Positive-ion electrospray ionization mass spectrometry (ESI(+))MS of a sample solution of cyclo[6]aramide **H1** and a pyridinium derivative **G1** in  $\text{CHCl}_3/\text{CH}_3\text{CN}$  (1:1, v/v) showed a dominant peak at  $m/z = 2444.3405$ , corresponding to the cation  $[\text{H1}_2 + \text{G1}_2 - 2\text{PF}_6^-]^{2+}$ , indicating the presence of a host–guest complex in a 2:2 stoichiometry in the gas state (Figure 1). Job plot experiments provided a 1:1 stoichiometry (Figure S9, Supporting Information File 3), showing consistency with the molar ratio observed in ESI experiments. These inspiring results prompted us to further examine the interaction between host **H1** and **G1** by  $^1\text{H}$  NMR spectroscopy. Our prior experience with cyclo[6]aramide has confirmed binding to the cationic guest [49]. Indeed, addition of compound **H1** to the guest solution resulted in a pronounced downfield shift ( $\Delta\delta = +0.694$  ppm) of protons  $\text{H}^1$  relative to the proton resonance of the free guest **G1** in  $\text{CDCl}_3/\text{CD}_3\text{CN}$  (1:1, v/v, Figure 2). Proton  $\text{H}^6$  also experienced a larger downfield shift ( $\Delta\delta = +0.519$  ppm). The fact that all other resonances for protons  $\text{H}^2$ – $\text{H}^5$  only showed relatively small lower frequency shifts ( $\Delta\delta = -0.033$ – $-0.270$  ppm) with respect to protons  $\text{H}^1$  and  $\text{H}^6$  suggested that the macrocycle tends to reside around the cationic pyridinium site in the binding process. On the other hand, the change in the chemical shift of the protons of **G1** was accompanied by a change in the resonance of the internal aromatic protons  $\text{H}^a$  and  $\text{H}^b$  in the host **H** ( $\Delta\delta = -0.170$  and  $+0.218$  ppm, respectively), which all pointed toward the existence of strong host–guest interactions in solution.

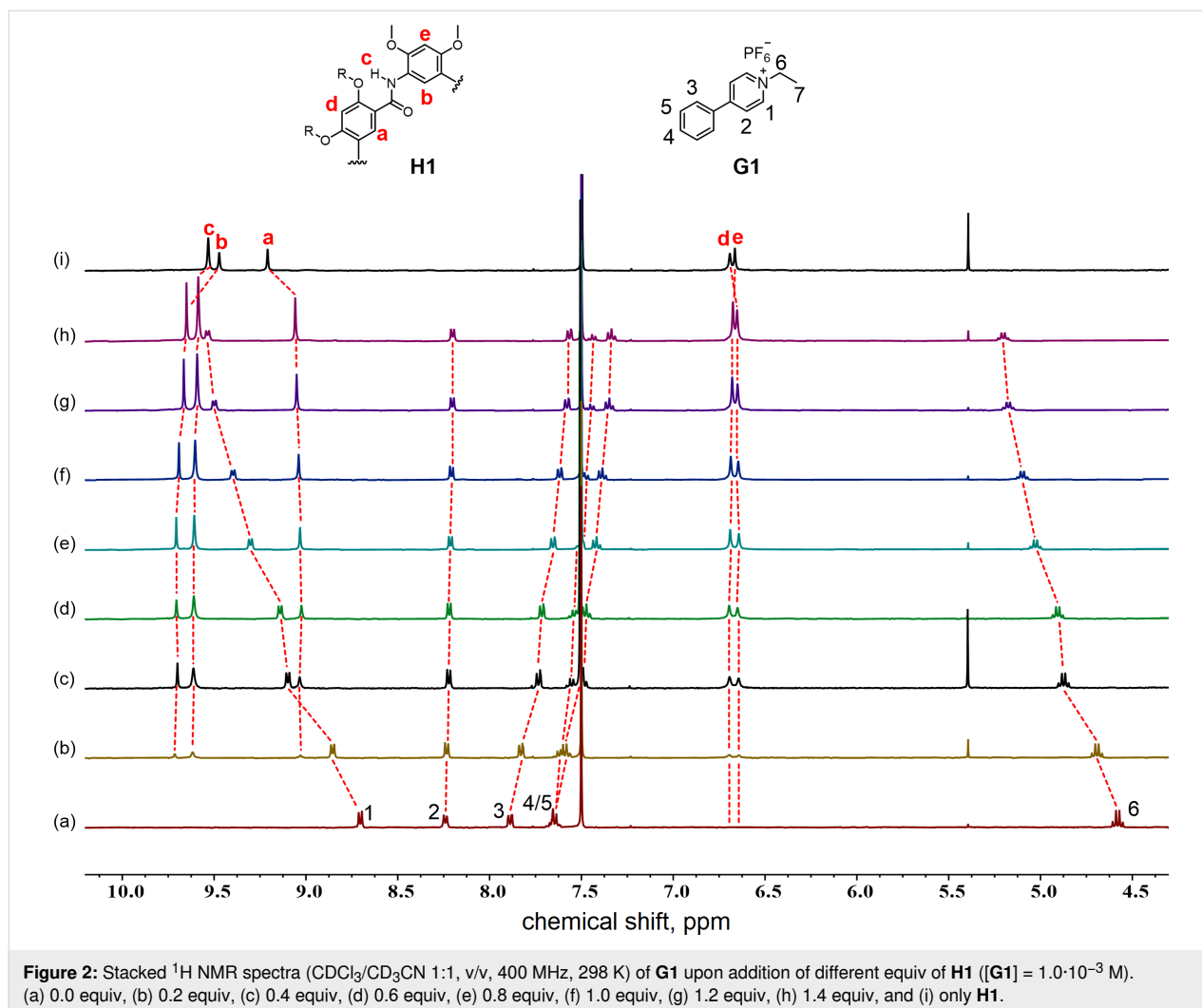
Then we attempted to grow single crystals of the complex out of curiosity, wondering whether the 2:2 structure would also be found in the solid state. Fortunately, single crystals of the complex **H1**  $\supset$  **G1** were obtained by slow evaporation of chloro-



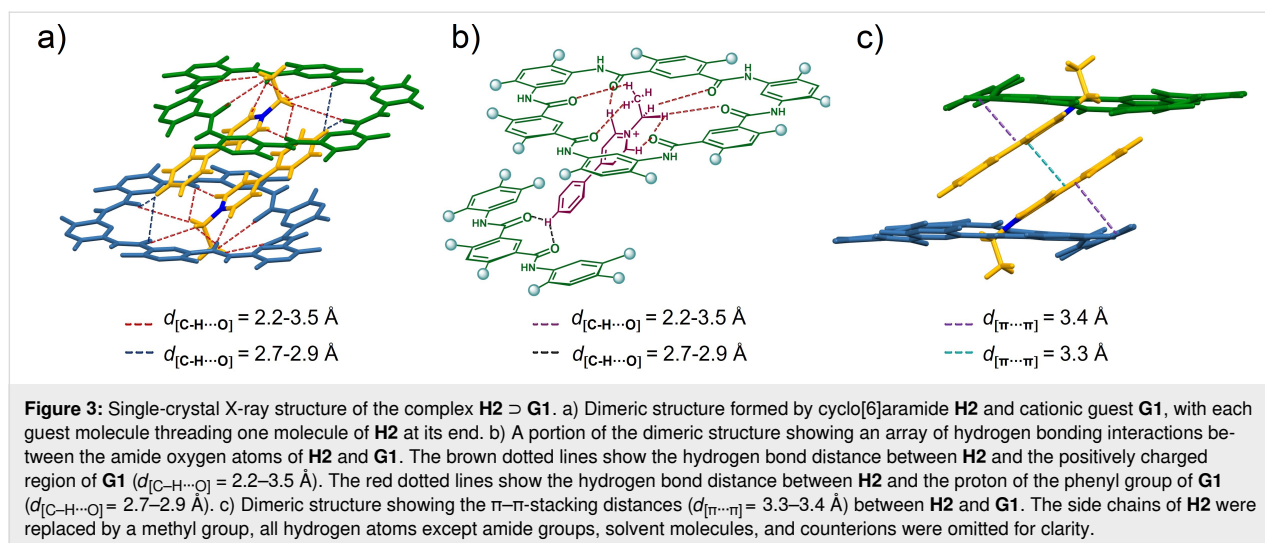
**Scheme 1:** a) Chemical structures of H-bonded macrocycles **H1**, **H2**, and guest **G1**, and schematic representation of the formation of a 2:2 host-guest complex. b) Chemical structure of guest **G2**. c) Schematic representation of the formation of a supramolecular polymer through orthogonal self-assembly upon addition of zinc ions.



form/acetone solvent (1:1, v/v) into a small amount of methanol over the course of two weeks. Indeed, analysis of the crystal structure of the complex revealed a strict 2:2 molar ratio (Figure 3), providing convincing evidence for the dimerization process. The complex crystallized in the monoclinic  $P2(1)/c$  space group with lattice constants  $a = 24.434(4)$  Å,  $b = 20.026(3)$  Å, and  $c = 23.779(4)$  Å. The dimeric superstructure was stabilized by multiple cooperative noncovalent interactions, particularly intermolecular  $\pi$ - $\pi$ -stacking and C-H $\cdots$ O interactions. Specifically,  $\pi$ - $\pi$ -stacking interactions were found between two guest molecules with aromatic rings arrayed in an offset fashion with a distance of 3.3 Å (Figure 3a). Interestingly, these interactions also existed between one guest and one phenyl ring of the host with a distance of 3.4 Å. The observation of these short  $\pi$ -distances suggested the crucial role of  $\pi$ -stacking interactions in sustaining the stability of the 2:2 complex of host **H2** and guest **G1**. It is worth mentioning that each of the two macrocycles adopted a nonplanar conformation, with one aromatic residue protruding out of the macrocyclic skeleton







plane. Adopting such a conformation rendered it possible for the  $\pi$ -electron-rich phenyl ring to interact strongly with  $\pi$ -electron-deficient guest molecules **G1** by means of charge–transfer interactions and/or  $\pi$ -stacking interactions, conferring the characteristic 2:2 constitutional stoichiometry onto this host–guest complex. In addition, there were eight C–H $\cdots$ O interactions between the hydrogen atoms of **G1** and the nearby pyridinium group of **H2**, with distances of 2.2–3.5 Å, and two C–H $\cdots$ O interactions between hydrogen atoms of **G1** and the nearby phenyl groups of **H2**, with a distance of 2.7–2.9 Å (Figure 3a and Figure 3b). These results provided conclusive evidence for the 2:2 recognition mode through interaction of two guests with two macrocycles.

With the 2:2 host–guest complexation pattern in mind, a guest molecule **G2** consisting of phenylpyridinium and a terpyridyl group was designed (Scheme 1b) to form a host–guest complex with cyclo[6]aramide **H1**. Compound **G2** was synthesized by refluxing **S2** and 4-phenylpyridine in acetonitrile for 24 h (Scheme S2, Supporting Information File 3). It was expected that by applying the design rules commonly known for metallo-supramolecular polymers and macrocycle-mediated dimerization to supramolecular chemistry, we would be able to generate supramolecular polymers with this heterodifunctional monomer, with one end comprising two macrocycles and the other end coordinating metal ions. In such supramolecular polymers, orthogonal host–guest and coordination interactions are responsible for polymerization.

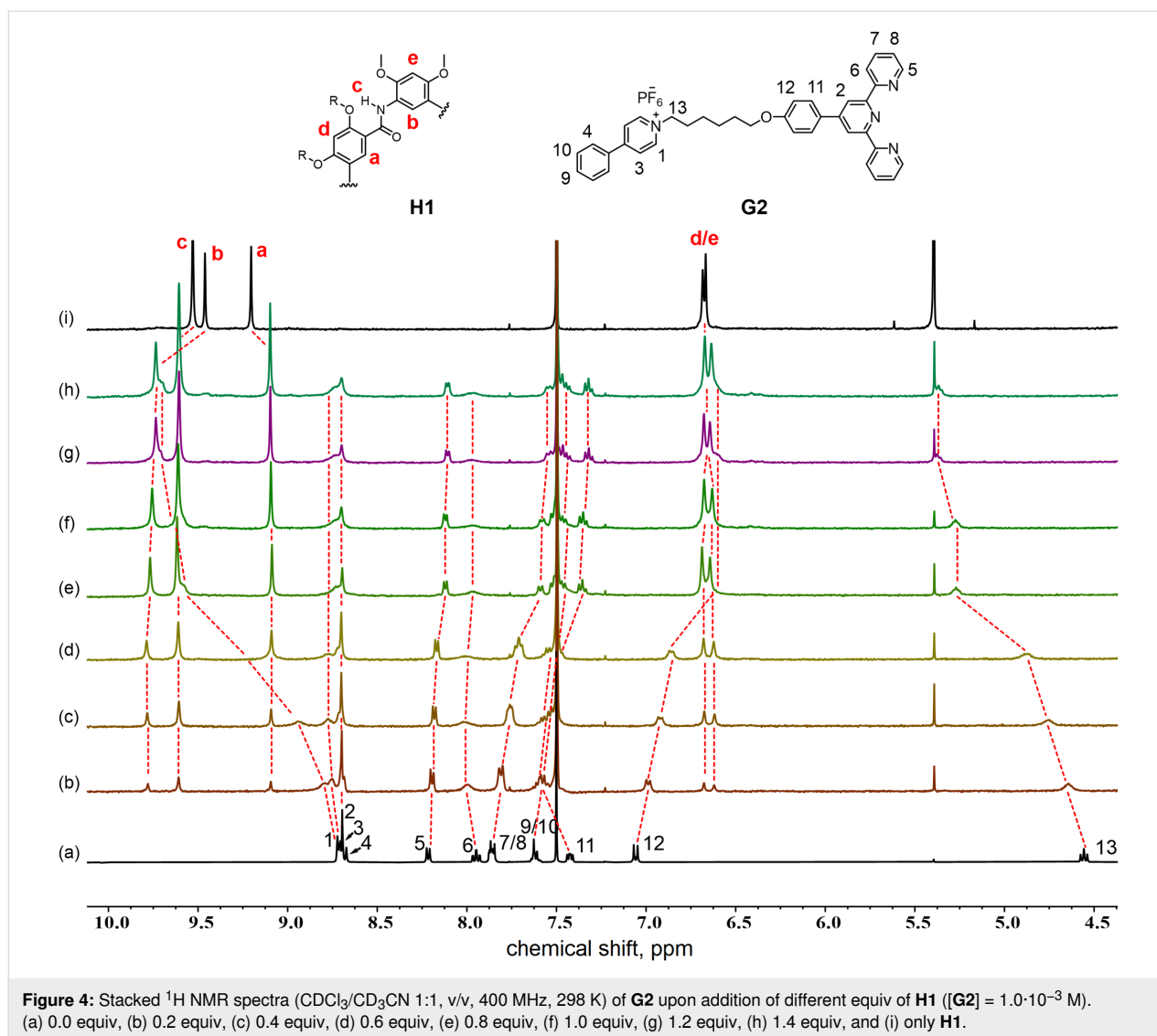
### Host–guest complexation and zinc coordination

When forming supramolecular polymers, an AB-type monomer, i.e., the guest **G2**, is supposed to interact with the macrocycle **H1** and a metal ion via each of two end groups (pyridinium and

terpyridyl). As such, host–guest complexation and zinc coordination of the AB-type monomer were investigated.

To begin with, the complex formation between host **H1** and **G2** was explored by  $^1\text{H}$  NMR spectroscopic titrations in  $\text{CDCl}_3/\text{CD}_3\text{CN}$  1:1, v/v. Titration of compound **H1** to the guest solution resulted in a constant downfield shift of protons  $\text{H}^1$  ( $\Delta\delta = +0.889\text{ ppm}$ ) and  $\text{H}^{13}$  ( $\Delta\delta = +0.716\text{ ppm}$ ) of the pyridinium moiety, signifying the complexation of the macrocycle at the cationic recognition site. The change in the chemical shift of  $\text{H}^{12}$  ( $\Delta\delta = -0.416\text{ ppm}$ ) could be explained by ring translocation along the guest axle due to dynamics in the binding process, which is often observed in pseudorotaxanes [50]. When the **H1/G2** molar ratio reached 1:1, the original proton signals of the macrocycle disappeared completely (Figure 4). Further addition of the macrocycle marginally influenced the new set of signals, suggesting formation of an  $n:n$  complex of **H1** and **G2**. Job plot experiments afforded a stoichiometry of  $n:n$  (Figure S10, Supporting Information File 3), purporting the probability of 2:2 complexation in solution. A strong indication of the formation of 2:2 complex came from ESIMS experiments. The mass spectra recorded for a 1:1 mixture of **H1** and **G2** showed a multicharged pseudomolecular ion peak corresponding to  $[\text{H1}_2 + \text{G2}_2 + \text{H}^+ - 2\text{PF}_6^-]^{3+}$ , and the isotope patterns were in good agreement with theoretical simulations (Figure S12, Supporting Information File 3). Therefore, taken together, these experimental results indicated that the macrocycle **H1** had a strong propensity for forming a 2:2 stoichiometric complex with guest **G2**.

The ability to coordinate with zinc ions constitutes another important aspect of orthogonal self-assembly. To this end, a mixture of **G2** and zinc salt in  $\text{CHCl}_3/\text{CH}_3\text{CN}$  (1:1, v/v) was subjected to  $^1\text{H}$  NMR spectroscopy. Protons  $\text{H}^2\text{--H}^4$ ,  $\text{H}^7$ ,  $\text{H}^8$ ,  $\text{H}^{11}$ ,



and  $\text{H}^{12}$  of **G2**, located around the metal coordination site, were found to experience upfield or downfield shifts to a varying extent (Figure S8, Supporting Information File 3). Particularly noteworthy was the pronounced downfield shift ( $\Delta\delta = +0.886$  ppm) of the signal of proton  $\text{H}^1$ . The change in the chemical shift of the protons of the terpyridyl group suggested the coordination of zinc ion with the terpyridyl end. NOESY data of **H1**  $\supset$  **G2**, acquired in a  $\text{CDCl}_3/\text{CD}_3\text{CN}$  solvent mixture (1:1, v/v), disclosed numerous spatial NOE correlations between the internal aromatic protons  $\text{H}^{\text{a}}\text{--H}^{\text{c}}$  of **H1** and the protons  $\text{H}^1$ ,  $\text{H}^2$ ,  $\text{H}^5$ ,  $\text{H}^9$ ,  $\text{H}^{10}$ , and  $\text{H}^{13}$  of **G2** (Figure S13, Supporting Information File 3).

### Orthogonal self-assembly and supramolecular polymerization

The structure of **G2**, with one end interacting only with macrocycles and the other end coordinating only with metal ions,

dictates that self-assembly will occur upon addition of either macrocycle or metal ions. However, supramolecular polymerization is unlikely to be induced unless both are present – a propensity of orthogonal self-assembly. Indeed, when **G2** and zinc salt were mixed together in a 1:1 molar ratio, results from dynamic light scattering experiments showed that the average hydrodynamic diameter ( $D_{\text{h}}$ ) was 524 nm, and no particles of discernible size were observed for a mixture of the macrocycle **H1** and **G2**, or **H1** and the salt, whereas with a solution containing **G2**, **H1**, and zinc salt, the  $D_{\text{h}}$  of the aggregates abruptly increased to 2580 nm (Figure S15, Supporting Information File 3). These results strongly indicated that polymerization proceeded only when both macrocycles and metal ion were present. TEM images of a solution containing **H1**, **G2**, and  $\text{Zn}^{2+}$  with a respective concentration of 1 mM and 3 mM revealed a nanoglobular suprastructure, and a larger nanoirregular block suprastructure at higher concentration (5 mM, Figure 5).

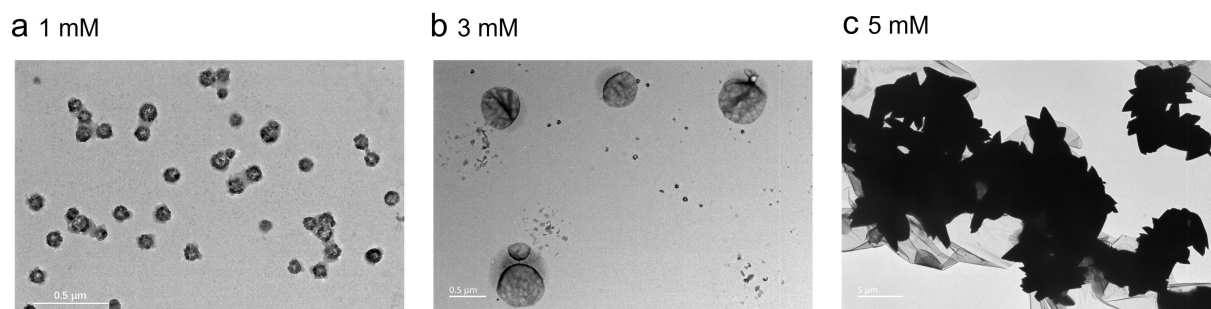


**Figure 5:** TEM images of a solution of **H1**, **G2**, and  $\text{Zn}(\text{ClO}_4)_2$  at different concentrations ( $\text{CHCl}_3/\text{CH}_3\text{CN}$  1:1, v/v, 298 K).

To confirm aggregate formation,  $^1\text{H}$  NMR titration experiments were carried out, in which different equiv of the macrocycle **H1** were added to a solution containing a 1:1 mixture of **G2** and zinc salt. Aromatic protons  $\text{H}^a$  ( $\Delta\delta = -0.142$  ppm) and  $\text{H}^b$  ( $\Delta\delta = +0.357$  ppm) were shifted downfield to a great extent, accompanied by the broadening of the signals of **G2** (Figure 6).

Constant downfield shifts were observed for protons  $\text{H}^1$  ( $\Delta\delta = +0.332$  ppm) and  $\text{H}^{13}$  ( $\Delta\delta = +0.473$  ppm) as well as protons  $\text{H}^{10}$  ( $\Delta\delta = -0.397$  ppm) and  $\text{H}^{12}$  ( $\Delta\delta = +0.246$  ppm) of the pyridinium moiety, signifying the complexation of the macrocycle at the cationic recognition site. The changes in the chemical shift and the broadening of signals after addition of the macro-

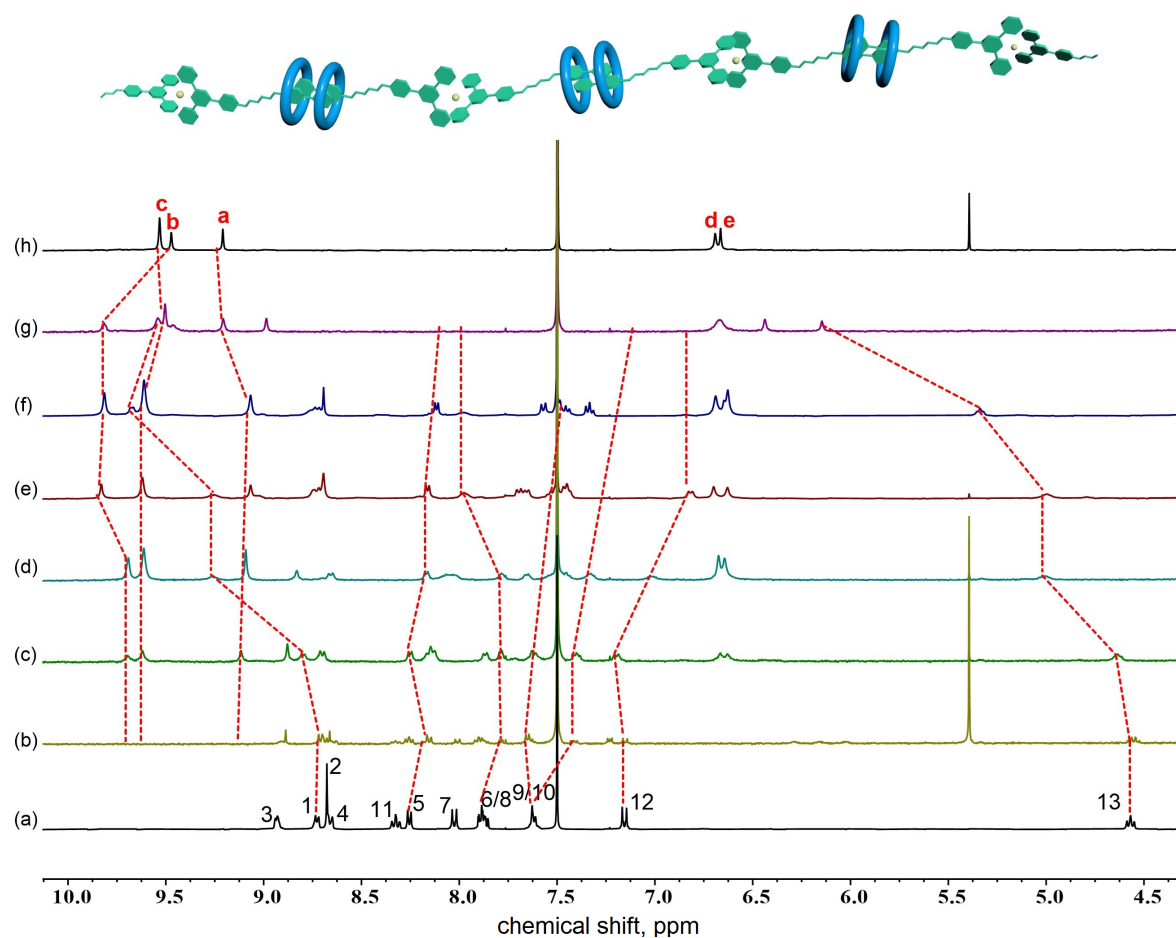


**Figure 6:** Stacked  $^1\text{H}$  NMR spectra ( $\text{CDCl}_3/\text{CD}_3\text{CN}$  1:1, v/v, 400 MHz, 298 K) of **G2** and  $\text{Zn}^{2+}$  upon addition of different equiv of **H1** ( $[\text{G2} + \text{Zn}^{2+}] = 1.0 \cdot 10^{-3}$  M). (a) 0.0 equiv, (b) 0.4 equiv, (c) 0.6 equiv, (d) 0.8 equiv, (e) 1.0 equiv, (f) 1.2 equiv, (g) 1.4 equiv, and (h) only **H1**.

cycle to a **G2**/ $\text{Zn}^{2+}$  complex were consistent with the formation of supramolecular polymers.

The supramolecular polymers formed were further characterized by viscosity and variable-concentration NMR experiments. One important feature of supramolecular polymers is the dependency of their molecular weight on the solution concentration. Further, a change in solution viscosity would reflect a change in molecular weight during the polymerization process. Thus, the specific viscosity of the linear supramolecular polymer (Scheme 1c) in  $\text{CHCl}_3/\text{CH}_3\text{CN}$  (1:1, v/v) was determined at 298 K (Figure 7). The specific viscosity was plotted against the concentration, which revealed two stages: prior to the turning point at 17  $\mu\text{M}$  and beyond. The first stage offered a slope of 1.1, corresponding to the formation of oligomeric assemblies in solution. On continuously increasing the concentration beyond 17  $\mu\text{M}$ , a second stage started, with a slope of 3.4, which is usually an indication of the formation of linear supramolecular polymers [51]. The observation of the turning point concentration, or of a critical polymerization concentration (CPC) [52,53], indicated concentration-driven polymerization, which is characteristic for the formation of supramolecular polymers. The concentration-dependency of a mixture of **H1**, **G2**, and zinc salt was examined by variable-concentration NMR spectroscopy. Pronounced broadening of signals was observed (Figure 8),

which clearly indicated increasing polymerization upon increasing the concentration of each component.

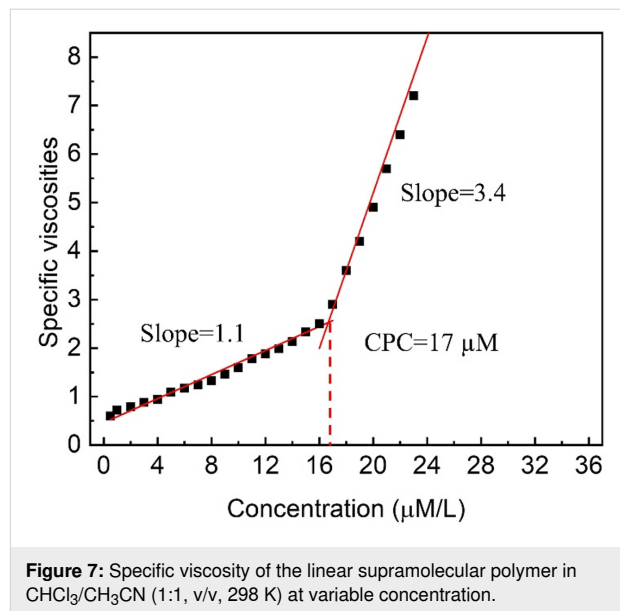


**Figure 7:** Specific viscosity of the linear supramolecular polymer in  $\text{CHCl}_3/\text{CH}_3\text{CN}$  (1:1, v/v, 298 K) at variable concentration.

## Conclusion

We have introduced a new recognition motif based on a hydrogen-bonded amide macrocycle, which drives the linear poly-

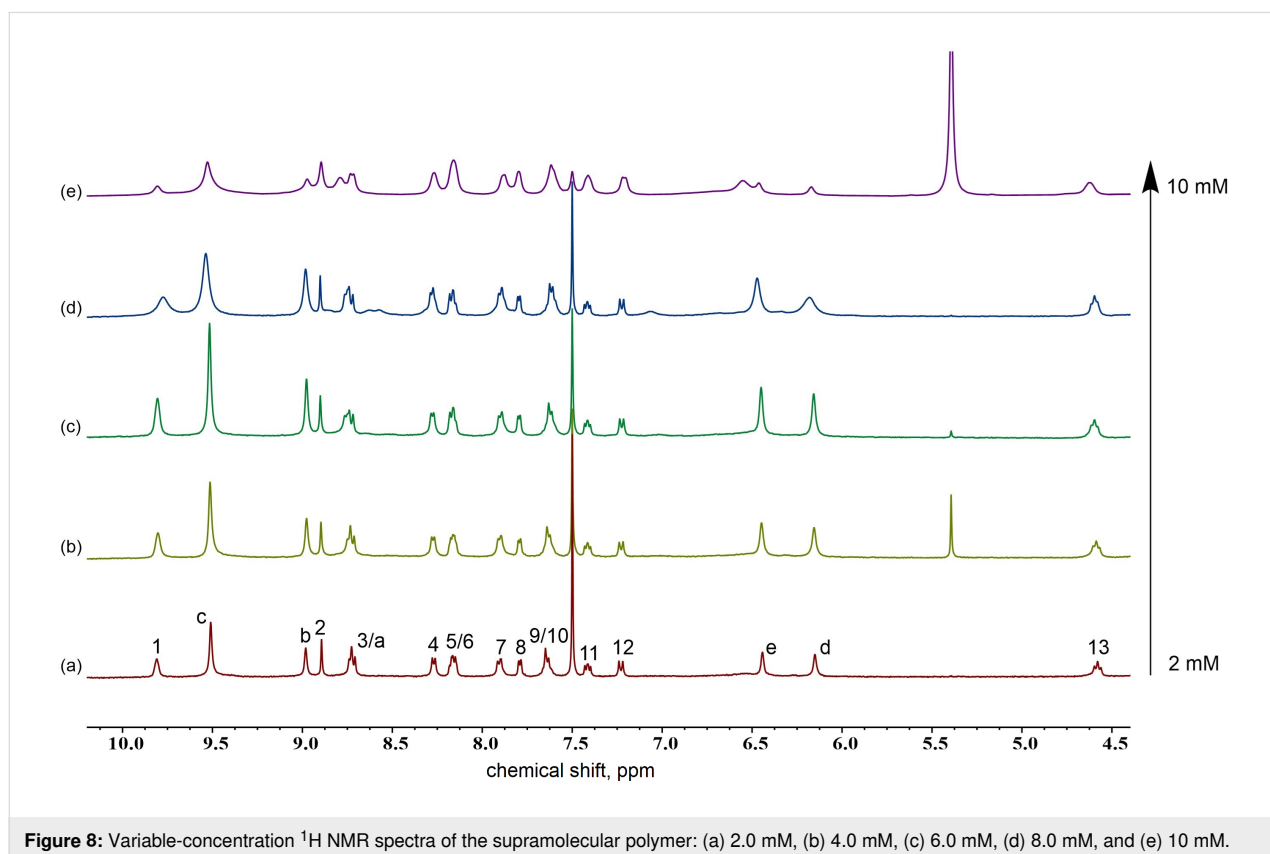


**Figure 8:** Variable-concentration  $^1\text{H}$  NMR spectra of the supramolecular polymer: (a) 2.0 mM, (b) 4.0 mM, (c) 6.0 mM, (d) 8.0 mM, and (e) 10 mM.

merization of a heterodifunctional monomer in the presence of zinc ions. In addition to hydrogen bonding interactions, the 2:2 host–guest dimerization is primarily facilitated by enhanced  $\pi$ -stacking interactions between the guests and between the guest and macrocycle. This 2:2 connectivity mode makes shape-persistent H-bonded macrocycles a valuable component for creating orthogonal supramolecular polymers, offering promising potential for designing stimuli-responsive and smart polymers in the future.

## Supporting Information

### Supporting Information File 1

CheckCIF report for **H2**  $\supset$  **G1**.

[<https://www.beilstein-journals.org/bjoc/content/supplementary/1860-5397-21-10-S1.pdf>]

### Supporting Information File 2

Crystallographic data for **H2**  $\supset$  **G1** analysed with SHELX (CCDC 2384953).

[<https://www.beilstein-journals.org/bjoc/content/supplementary/1860-5397-21-10-S2.cif>]

### Supporting Information File 3

Experimental data and copies of spectra.

[<https://www.beilstein-journals.org/bjoc/content/supplementary/1860-5397-21-10-S3.pdf>]

## Acknowledgements

We thank Dr. Dongyan Deng from the College of Chemistry as well as Dr. Pengchi Deng and Dr. Chen Yuan from The Analytical & Testing Center, Sichuan University, for analytic testing and valuable help.

## Funding

This research was financially supported by the National Natural Science Foundation of China (22271202 to L. Yuan, 22201193 to X. Li), the Sichuan Science and Technology Program (2023NSFSC0109 to X. Li), the Fundamental Research Funds for the Central Universities and the Hundred Talent Program of Sichuan University (YJ2021158 to X. Li), the Sichuan University Interdisciplinary Innovation Fund (X. Li), and Open Project of State Key Laboratory of Supramolecular Structure and Materials (SKLSSM2024037).

## Author Contributions

Wentao Yu: data curation; formal analysis; investigation; methodology; resources; writing – review & editing. Zhiyao Yang: data curation; formal analysis; methodology; visualization;

writing – review & editing. Chengkan Yu: data curation; formal analysis; visualization; writing – review & editing. Xiaowei Li: conceptualization; data curation; formal analysis; funding acquisition; methodology; project administration; resources; supervision; writing – original draft; writing – review & editing. Lihua Yuan: conceptualization; data curation; formal analysis; funding acquisition; project administration; resources; supervision; writing – original draft; writing – review & editing.

## ORCID® iDs

Wentao Yu - <https://orcid.org/0009-0006-7444-8248>

Zhiyao Yang - <https://orcid.org/0000-0001-7994-356X>

Chengkan Yu - <https://orcid.org/0009-0001-3514-3218>

Xiaowei Li - <https://orcid.org/0000-0001-9479-4857>

Lihua Yuan - <https://orcid.org/0000-0003-0578-4214>

## Data Availability Statement

All data that supports the findings of this study is available in the published article and/or the supporting information of this article.

## Preprint

A non-peer-reviewed version of this article has been previously published as a preprint: <https://doi.org/10.3762/bxiv.2024.62.v1>

## References

- Ji, X.; Ahmed, M.; Long, L.; Khashab, N. M.; Huang, F.; Sessler, J. L. *Chem. Soc. Rev.* **2019**, *48*, 2682–2697. doi:10.1039/c8cs00955d
- Yang, H.; Yuan, B.; Zhang, X.; Scherman, O. A. *Acc. Chem. Res.* **2014**, *47*, 2106–2115. doi:10.1021/ar500105t
- Yan, M.; Wu, S.; Wang, Y.; Liang, M.; Wang, M.; Hu, W.; Yu, G.; Mao, Z.; Huang, F.; Zhou, J. *Adv. Mater. (Weinheim, Ger.)* **2024**, *36*, 2304249. doi:10.1002/adma.202304249
- Yu, G.; Jie, K.; Huang, F. *Chem. Rev.* **2015**, *115*, 7240–7303. doi:10.1021/cr5005315
- Huck, W. T. S.; Hulst, R.; Timmerman, P.; van Veggel, F. C. J. M.; Reinhoudt, D. N. *Angew. Chem., Int. Ed. Engl.* **1997**, *36*, 1006–1008. doi:10.1002/anie.199710061
- Tian, X.; Zuo, M.; Niu, P.; Velmurugan, K.; Wang, K.; Zhao, Y.; Wang, L.; Hu, X.-Y. *ACS Appl. Mater. Interfaces* **2021**, *13*, 37466–37474. doi:10.1021/acsami.1c07106
- Wong, C.-H.; Zimmerman, S. C. *Chem. Commun.* **2013**, *49*, 1679–1695. doi:10.1039/c2cc37316e
- Wang, S.; Xu, Z.; Wang, T.; Xiao, T.; Hu, X.-Y.; Shen, Y.-Z.; Wang, L. *Nat. Commun.* **2018**, *9*, 1737. doi:10.1038/s41467-018-03827-3
- Wei, P.; Yan, X.; Huang, F. *Chem. Soc. Rev.* **2015**, *44*, 815–832. doi:10.1039/c4cs00327f
- Xiao, T.; Zhou, L.; Sun, X.-Q.; Huang, F.; Lin, C.; Wang, L. *Chin. Chem. Lett.* **2020**, *31*, 1–9. doi:10.1016/j.cclet.2019.05.011
- Hu, X.-Y.; Xiao, T.; Lin, C.; Huang, F.; Wang, L. *Acc. Chem. Res.* **2014**, *47*, 2041–2051. doi:10.1021/ar5000709
- Li, Y.; Lou, X.; Wang, C.; Wang, Y.; Jia, Y.; Lin, Q.; Yang, Y. *Chin. Chem. Lett.* **2023**, *34*, 107877. doi:10.1016/j.cclet.2022.107877
- Xu, L.; Chen, D.; Zhang, Q.; He, T.; Lu, C.; Shen, X.; Tang, D.; Qiu, H.; Zhang, M.; Yin, S. *Polym. Chem.* **2018**, *9*, 399–403. doi:10.1039/c7py01788j

14. Bai, Z.; Velmurugan, K.; Tian, X.; Zuo, M.; Wang, K.; Hu, X.-Y. *Beilstein J. Org. Chem.* **2022**, *18*, 429–437. doi:10.3762/bjoc.18.45
15. Samanta, S. K.; Quigley, J.; Vinciguerra, B.; Briken, V.; Isaacs, L. *J. Am. Chem. Soc.* **2017**, *139*, 9066–9074. doi:10.1021/jacs.7b05154
16. Wu, H.; Chen, Y.; Dai, X.; Li, P.; Stoddart, J. F.; Liu, Y. *J. Am. Chem. Soc.* **2019**, *141*, 6583–6591. doi:10.1021/jacs.8b13675
17. Yang, L.; Tan, X.; Wang, Z.; Zhang, X. *Chem. Rev.* **2015**, *115*, 7196–7239. doi:10.1021/cr500633b
18. Barrow, S. J.; Kasera, S.; Rowland, M. J.; del Barrio, J.; Scherman, O. A. *Chem. Rev.* **2015**, *115*, 12320–12406. doi:10.1021/acs.chemrev.5b00341
19. Xia, Z.; Song, Y.-F.; Shi, S. *Angew. Chem., Int. Ed.* **2024**, *63*, e202312187. doi:10.1002/anie.202312187
20. Budak, A.; Aydogan, A. *Chem. Commun.* **2021**, *57*, 4186–4189. doi:10.1039/d1cc01003d
21. Wei, P.; Yan, X.; Cook, T. R.; Ji, X.; Stang, P. J.; Huang, F. *ACS Macro Lett.* **2016**, *5*, 671–675. doi:10.1021/acsmacrolett.6b00286
22. Chen, Y.; Kuvayskaya, A.; Pink, M.; Sellinger, A.; Flood, A. H. *Chem. Sci.* **2024**, *15*, 389–398. doi:10.1039/d3sc03685e
23. Zhao, W.; Qiao, B.; Tropp, J.; Pink, M.; Azoulay, J. D.; Flood, A. H. *J. Am. Chem. Soc.* **2019**, *141*, 4980–4989. doi:10.1021/jacs.9b00248
24. Yu, H.-J.; Zhou, X.-L.; Dai, X.; Shen, F.-F.; Zhou, Q.; Zhang, Y.-M.; Xu, X.; Liu, Y. *Chem. Sci.* **2022**, *13*, 8187–8192. doi:10.1039/d2sc02384a
25. Olesińska, M.; Wu, G.; Gómez-Coca, S.; Antón-García, D.; Szabó, I.; Rosta, E.; Scherman, O. A. *Chem. Sci.* **2019**, *10*, 8806–8811. doi:10.1039/c9sc03057c
26. Tang, B.; Xu, W.; Xu, J.-F.; Zhang, X. *Angew. Chem., Int. Ed.* **2021**, *60*, 9384–9388. doi:10.1002/anie.202100185
27. Yang, X.; Wang, R.; Kermagoret, A.; Bardelang, D. *Angew. Chem., Int. Ed.* **2020**, *59*, 21280–21292. doi:10.1002/anie.202004622
28. Zhang, X.-D.; Fang, F.; Chen, K.; Ni, Y. *Dyes Pigm.* **2024**, *227*, 112181. doi:10.1016/j.dyepig.2024.112181
29. Xia, D.; Wang, P.; Ji, X.; Khashab, N. M.; Sessler, J. L.; Huang, F. *Chem. Rev.* **2020**, *120*, 6070–6123. doi:10.1021/acs.chemrev.9b00839
30. Wu, G.; Li, F.; Tang, B.; Zhang, X. *J. Am. Chem. Soc.* **2022**, *144*, 14962–14975. doi:10.1021/jacs.2c02434
31. Zhang, W.; Moore, J. S. *Angew. Chem., Int. Ed.* **2006**, *45*, 4416–4439. doi:10.1002/anie.200503988
32. Höger, S. *Chem. – Eur. J.* **2004**, *10*, 1320–1329. doi:10.1002/chem.200305496
33. Li, X.; Li, B.; Chen, L.; Hu, J.; Wen, C.; Zheng, Q.; Wu, L.; Zeng, H.; Gong, B.; Yuan, L. *Angew. Chem., Int. Ed.* **2015**, *54*, 11147–11152. doi:10.1002/anie.201505278
34. Klyatskaya, S.; Dingenouts, N.; Rosenauer, C.; Müller, B.; Höger, S. *J. Am. Chem. Soc.* **2006**, *128*, 3150–3151. doi:10.1021/ja057999g
35. Gomez, E.; di Nunzio, M. R.; Moreno, M.; Hisaki, I.; Douhal, A. *J. Phys. Chem. C* **2020**, *124*, 6938–6951. doi:10.1021/acs.jpcc.0c01369
36. Gong, B.; Shao, Z. *Acc. Chem. Res.* **2013**, *46*, 2856–2866. doi:10.1021/ar400030e
37. Ong, W. Q.; Zeng, H. J. *Inclusion Phenom. Macrocyclic Chem.* **2013**, *76*, 1–11. doi:10.1007/s10847-012-0243-4
38. Zhang, D.-W.; Zhao, X.; Hou, J.-L.; Li, Z.-T. *Chem. Rev.* **2012**, *112*, 5271–5316. doi:10.1021/cr300116k
39. Liu, Z.; Zhou, Y.; Yuan, L. *Org. Biomol. Chem.* **2022**, *20*, 9023–9051. doi:10.1039/d2ob01263d
40. Huang, S.; Li, X.; Cai, Y.; Feng, W.; Yuan, L. *Chem. – Eur. J.* **2024**, *30*, e202303394. doi:10.1002/chem.202303394
41. Lu, K.; Zhang, P.; Yue, Y.; Yuan, X.; Yuan, L.; Feng, W. *Przem. Chem.* **2017**, *96*, 1906–1912.
42. Zhu, Y.; Chen, C.; Sangaraiah, N.; Kannekanti, V. K.; Yuan, L.; Feng, W. *J. Iran. Chem. Soc.* **2018**, *15*, 2861–2869. doi:10.1007/s13738-018-1472-2
43. Ren, C.; Shen, J.; Zeng, H. *Org. Lett.* **2015**, *17*, 5946–5949. doi:10.1021/acs.orglett.5b02780
44. Helsel, A. J.; Brown, A. L.; Yamato, K.; Feng, W.; Yuan, L.; Clements, A. J.; Harding, S. V.; Szabo, G.; Shao, Z.; Gong, B. *J. Am. Chem. Soc.* **2008**, *130*, 15784–15785. doi:10.1021/ja807078y
45. Kang, K.; Lohrman, J. A.; Nagarajan, S.; Chen, L.; Deng, P.; Shen, X.; Fu, K.; Feng, W.; Johnson, D. W.; Yuan, L. *Org. Lett.* **2019**, *21*, 652–655. doi:10.1021/acs.orglett.8b03778
46. Huang, S.; Wang, Z.; Wu, J.; Mai, X.; Qin, S.; Zhou, Y.; Yuan, D.; Li, X.; Feng, W.; Yuan, L. *Chem. Commun.* **2024**, *60*, 5622–5625. doi:10.1039/d4cc00178h
47. Yang, Z.; Wang, X.; Penocchio, E.; Ragazzon, G.; Chen, X.; Lu, S.; Zhou, Y.; Fu, K.; Liu, Z.; Cai, Y.; Yu, X.; Li, X.; Li, X.; Feng, W.; Yuan, L. *Angew. Chem., Int. Ed.* **2025**, *64*, e202414072. doi:10.1002/anie.202414072
48. Xu, M.; Chen, L.; Jia, Y.; Mao, L.; Feng, W.; Ren, Y.; Yuan, L. *Supramol. Chem.* **2015**, *27*, 436–443. doi:10.1080/10610278.2014.1002840
49. Yu, W.; Kothapalli, S. S. K.; Yang, Z.; Guo, X.; Li, X.; Cai, Y.; Feng, W.; Yuan, L. *Molecules* **2024**, *29*, 4842. doi:10.3390/molecules29204842
50. Wang, Q.; Zhang, P.; Li, Y.; Tian, L.; Cheng, M.; Lu, F.; Lu, X.; Fan, Q.; Huang, W. *RSC Adv.* **2017**, *7*, 29364–29367. doi:10.1039/c7ra05351g
51. Wu, L.; Han, C.; Wu, X.; Wang, L.; Caochen, Y.; Jing, X. *Dalton Trans.* **2015**, *44*, 20334–20337. doi:10.1039/c5dt04237b
52. Scherman, O. A.; Ligthart, G. B. W. L.; Sijbesma, R. P.; Meijer, E. W. *Angew. Chem., Int. Ed.* **2006**, *45*, 2072–2076. doi:10.1002/anie.200504192
53. Liu, Y.; Wang, Z.; Zhang, X. *Chem. Soc. Rev.* **2012**, *41*, 5922. doi:10.1039/c2cs35084j

## License and Terms

This is an open access article licensed under the terms of the Beilstein-Institut Open Access License Agreement (<https://www.beilstein-journals.org/bjoc/terms>), which is identical to the Creative Commons Attribution 4.0 International License (<https://creativecommons.org/licenses/by/4.0>). The reuse of material under this license requires that the author(s), source and license are credited. Third-party material in this article could be subject to other licenses (typically indicated in the credit line), and in this case, users are required to obtain permission from the license holder to reuse the material.

The definitive version of this article is the electronic one which can be found at:  
<https://doi.org/10.3762/bjoc.21.10>